American Mineralogist, Volume 71, pages 111–122, 1986

Nature of phases synthesized along the join $(Mg,Mn)_2Si_2O_6$

J. Stephen Huebner

U.S. Geological Survey, Reston, Virginia 22092

Abstract

Eight compositions were synthesized along the join. Orthopyroxene crystallized at X = Mn/(Mn + Mg) = 0.0–0.3, clinopyroxene at X = 0.4–0.5, and pyroxmangite at X = 0.65–1.0, consistent with the composition ranges that have been inferred by examination of metamorphic rock assemblages. Unit cell dimensions for these phases and for rhodonite (X = 1.0) are presented. Microprobe chemical analyses reveal that compositional homogeneity was not always achieved, even in runs at 850°C and 1 kbar water pressure lasting 1000–2000 hours. For the bulk composition range X = 0.0–0.3, below 725°C, clinoamphibole and/or talc occurred instead of orthopyroxene. Diagrams are used to suggest possible phase relations among the metasilicates, cummingtonite or anthophyllite, olivine, and talc.

Introduction

Fifteen years ago I attempted to synthesize amphiboles along the join Mg-cummingtonite, $Mg_7Si_8O_{22}(OH)_2$, to Mn-Mg-amphibole, $(Mg,Mn)_7Si_2O_{22}(OH)_2$. Few run products contained more than a 95% yield of amphibole, so the results did not contribute much to the knowledge of amphibole crystal chemistry. Products of the highest temperature runs, usually a metasilicate plus quartz, demonstrated extensive solid solution between enstatite, $Mg_2Si_2O_6$, and Mn-pyroxene component. I prepared manganese-rich bulk compositions with the thought that I might encounter a succession of pyroxenoid minerals with repeats (along the silicate chain) varying from 5 at the $MnSiO_3$ endmember to infinite at the more magnesian orthopyroxene. Many of the peaks observed in X-ray diffractometer patterns of the low-symmetry, manganese-rich compositions were not sharp, most probably because these peaks were composites of several reflections. I had great difficulty indexing these patterns and set the study aside rather than report the synthesis of poorly characterized phases. The paper on the Mg-Mn orthopyroxene donpeacorite, $(Mg,Mn)Si_2O_6$, by Petersen et al. (1984) describes one of the phases that I had synthesized. The opportunity to review this paper for the American Mineralogist and the authors' appeal for experimental data at metamorphic temperatures prodded me to look again at my run products.

Just as the first draft of this manuscript was being completed, Maresch and Czank (1983) published a paper on the phase characterization of $(Mn,Mg)_7Si_8O_{22}(OH)_2$ amphiboles—the same join on which I had originally focused my attention. Rather than use high resolution electron microscopy techniques to explore whether or not Maresch and Czank duplicated my amphibole-bearing runs, I will present a comparison only of the results obtained by optical microscopy and X-ray diffraction.

Naturally occurring orthopyroxene, $(Mg,Fe)Si_2O_6$, commonly contains not more than 0.08 cations of manganese per 6-oxygen formula unit (Robinson, 1980). On the basis of natural manganiferous assemblages, Brown et al. (1980) inferred that magnesian orthopyroxene solid solution did not extend farther toward $Mn_2Si_2O_6$ than $Mn_{0.2}Mg_{1.8}Si_2O_6$. They show that orthopyroxene of this composition coexists with kanoite, a clinopyroxene with approximate composition $MnMgSi_2O_6$. Kanoite occurs in manganiferous layers of a gneiss metamorphosed to hornblende hornfels grade (Kobayashi, 1977) and with magnesium rhodonite in manganiferous pods metamorphosed at 625°C and 6.5 kbar peak conditions (Gordon et al., 1981). The occurrence of kanoite with rhodonite suggests that the clinopyroxene cannot have a Mn/(Mn + Mg) ratio (X) exceeding X = 0.5, at least at the metamorphic conditions recorded in the associated rocks. The description of donpeacorite extends the known natural orthopyroxene solid solution range to X = 0.3, narrowing the range of possible kanoite compositions in the Mg-Mn system to X = 0.3–0.5. The composition of the magnesium rhodonite coexisting with kanoite is not known but can be inferred to be X = 0.9 from Petersen et al. (1984, Fig. 4). Where, at other localities, the pyroxenoid coexisting with kanoite is pyroxmangite, the pyroxenoid composition can be as magnesian as X = 0.7 (Brown et al., 1980; Petersen et al., 1984).

Previous published experimental work on the binary system is summarized by Ito (1972) who synthesized, with increasing X at high temperature (approximately 1300°C) in air, the sequence of phases protopyroxene, clinopyroxene, pyroxmangite, and rhodonite. Pyroxmangite occupies the composition range X = 0.10–1.00 whereas rhodonite occurs only over the range X = 0.55–1.00. From Ito's synthesis diagram one can infer that, within the rhodonite composition range, and at temperatures exceeding

0003–004X/86/0102–0111$02.00

1200°C, the rhodonite structure is preferred over that of pyroxmangite. This high-temperature synthesis diagram does not show composition limits that agree with the phase relations that have been inferred from natural assemblages.

Phase assemblages in the system MgO-SiO_2-H_2O were determined by Hemley et al. (1977) who found that at a silica activity near unity and at the pressures of the present study, first enstatite is replaced by anthophyllite, then anthophyllite by talc, as temperature decreases. Reactions involving magnesian cummingtonite have not been investigated but are assumed to be similar.

The end-member composition $MnSiO_3$ can exist with either the rhodonite or the pyroxmangite structure at low pressure. Maresch and Mottana (1976) have shown that, over the pressure range 3.5 to 30 kbar, pyroxmangite is the stable low-temperature polymorph and rhodonite is stable at higher temperature. Their results are consistent with the results of Akimoto and Syono (1972) at even higher pressures. When extrapolated to lower pressure, the trend of these data suggests that at 1 to 2 kbar pressure, the pyroxmangite-rhodonite inversion lies at 400°C.

Experimental methods

Compositions along the amphibole join $Mg_7Si_8O_{23}$-$Mn_5Mg_2Si_8O_{23}$ and the compositions $MnMgSi_2O_6$ and $Mn_2Si_2O_6$ were prepared from reagent grade MgO (Fisher Lot 787699), MnO_2 (Baker Lots 22587 and 30740), and SiO_2 (ignited and acid-washed Corning silica glass cullet 7940 or, for $MnSiO_3$ composition only, natural quartz) and mixed by grinding for 0.5–1.0 hour in an agate mortar. Manganese-bearing mixes were reduced in hydrogen at approximately 650°C so that all manganese was sensibly in the divalent state. (The stability field of "MnO" in temperature-oxygen fugacity space is much larger than the "FeO" field; see fig. 3 of Huebner, 1969.) The mixes were crystallized in unbuffered O-H or buffered O-H and C-O-H fluids using techniques reviewed by Huebner (1971). In most runs, the water formed less than 20 wt.% of the charge. In one run, large rhodonite crystals were crystallized in a molten $MnCl_2$ flux. For the unbuffered syntheses, the hydrogen fugacity was established by the walls of the pressure vessel and is believed to be close to values that would have been established by the Ni-NiO buffer, had it been used. Many runs were of unusually long duration (in an attempt to grow large single crystals). The run products are well crystallized and appear to represent at least a steady state if not an equilibrium state.

All run products were examined with the optical microscope and with the X-ray powder diffractometer using standard methods. The metasilicates are coarse-grained and, with practice, can be readily distinguished optically by observing the crystal habit and extinction angle. As a rule, run products containing amphibole or talc are so fine-grained that optical microscopy did not result in definitive identification. Likewise, the X-ray diffractometer patterns of the metasilicates were distinct and can be indexed by analogy with published patterns of hypersthene (Borg and Smith, 1969), kanoite (Kobayshi, 1977), and pyroxmangite (Maresch and Mottana, 1976), but the patterns containing amphibole and talc contain few reflections, many of which were weak and broad. To identify the amphibole, the patterns were compared with published patterns for manganoan cummingtonite, anthophyllite, and protoamphibole (Klein, 1964; Cameron, 1975; Borg and Smith, 1969).

Unit cell dimensions were obtained using Cu$K\alpha$ radiation and BaF_2, αAl_2O_3, NaF, and Si as internal standards. For most measurements, the diffractometer scanned continuously from 70 down to 20 or 10° 2θ. Count data were repeatedly digitized (pulses were counted for 0.005° 2θ, equivalent to 1.2 seconds, of scan, then the number of pulses was written on computer-readable magnetic tape). Corrected 2θ values were obtained using USGS Program 9208 (see Huebner and Papike, 1970). Some recent 2θ measurements were made with a Philips APD3600 automated powder diffractometer[1] and corrected with software provided with the instrument. These recent results agree with the previous results. Unit cell constants were calculated using only unambiguously indexed reflections as input for the least-squares refinement program of Evans et al. (1963). The misfit between the values of observed reflections and values calculated from the refined cell can be expressed in terms of a standard error in 2θ; values of less than 0.015° are unusually good, whereas values greater than 0.20° are disappointing. Values encountered in this study ranged from 0.012 to 0.030° 2θ.

Representative run products were chemically analysed with an Applied Research Laboratories EMX electron microprobe operated at 15 kV and 100 nA beam current, using a Kreisel wavelength-dispersive automation system (Finger and Hadidiacos, 1972) and a 20 second count time. The standards for analysis were synthetic enstatite (PXSE, $MgSiO_3$) for Mg and Si and synthetic tephroite (OLST, Mn_2SiO_4) for Mn. Oxide concentration values were corrected using the scheme of Bence and Albee (1968) and the correction factors of Albee and Ray (1970).

Results

The products of the syntheses at temperatures greater than 750°C are metasilicates plus, for the amphibole bulk compositions, quartz (Table 1). The colors of the charges change progressively with composition from white (enstatite) to very pale pink (manganiferous orthopyroxene) to deep pink (pyroxenoids of $MnSiO_3$ composition). In long runs, orthopyroxene and kanoite acquired an acicular habit with crystals as long as 350 and 90 μm, respectively. These crystals are too slender to be suitable for conventional single crystal X-ray diffraction techniques; no pyroxene crystal exceeded 50 μm in its next greatest dimension. The orthopyroxene crystals are invariably simple crystals with parallel extinction whereas kanoite crystals are commonly twinned and have an extinction angle (42°) that is comparable to that of pigeonite, the low-calcium pyroxene analogue. Pyroxenoids characteristically form masses of equant subhedral or anhedral crystals. In the relatively rare cases of well-developed crystal form, the crystal length does not exceed 40 μm. These crystals, grown hydrothermally from a reduced oxide mix, have sharp extinction in contrast to much longer curved sheaves of pyroxmangite crystals grown from a rhodochrosite + quartz mix in a carbon dioxide-rich atmosphere (Huebner, 1967).

With increasing manganese content the synthesis field of orthopyroxene gives way to orthopyroxene + kanoite (inferred field, Fig. 1a), kanoite, kanoite + pyroxenoid, and pyroxenoid (rhodonite, pyroxmangite). Rhodonite was

[1] The use of trade names is for descriptive purposes only and does not imply endorsement by the U.S. Geological Survey.

Table 1. Experimental runs in the system $MgSiO_3$-$MnSiO_3$-SiO_2-fluid

Run	°C	kb	hrs	Buffer	Mn/(Mg+Mn)	Reactants	Products
43	815	1.0	5418	Au capsule	0.0	MgO,SiO_2,H_2O	Opx,Qtz
45	825	1.0	4779	"	0.0	"	"
5	463	2.0	2204	"	0.143	MgO,MnO,SiO_2,H_2O	Tc
7	650	2.0	162	"	"	"	Tc,Amph
10	up to 879	2.0	168	"	"	"	Opx,Qtz
12	798	1.0	1680	"	"	"	Opx,Qtz
30	800	1.0	2112	"	"	"	Opx,Qtz
31	670	1.0	435	"	"	Opx+Qtz(12),H_2O	Opx,Amph,Tc
37	656	1.0	5022	"	"	Opx+Qtz(30),H_2O	Opx,Qtz
1	520	2.0	233	"	0.0286	MgO,MnO,SiO_2,H_2O	Amph,Tc,20%
2	710	2.0	65	"	"	"	Amph,10%
4	709	2.0	120	"	"	"	Amph
6	463	2.0	2204	"	"	"	Tc,5%,10%
8	650	2.0	162	"	"	"	Amph
9	771,879	2.0	168	"	"	"	Opx,Qtz
11	789	1.0	1680	"	"	"	Opx,Qtz
13	634	2.0	1320	"	"	"	Amph
15	789	0.5	186	"	"	"	Opx,Qtz
19	808	1.0	74	"	"	"	Opx,Qtz
23	694	1.0	621	"	"	"	Amph,Pxn?
25	775	1.0	791	"	"	"	Opx,Qtz
29	805	1.0	2813	"	"	"	Opx,Qtz
35	800	1.0	5355	"	"	"	Opx,Qtz
18	770	1.0	596	"	"	Amph(13),H_2O	Amph,Opx,Qtz
22	743	1.0	306	NNO,OH(X,OH)	"	Amph+Opx+Qtz,H_2O	Opx,Qtz
23	694	1.0	621	Au capsule	"	MgO,MnO,SiO_2,H_2O	Amph,Cpx?
24	783	1.0	95	WM,OH(X,OH)	"	Amph+Opx+Qtz,H_2O	Opx,Qtz
25	745,804	1.0	791	Au capsule	"	MgO,MnO,SiO_2,H_2O	Opx,Qtz,Amph
27	698	1.0	2329	NNO,OH(X,OH)	"	Opx+Q,H_2O	Opx+Q
28	641	≤2.0	312	"	"	Opx+Q,H_2O	Opx+Q+Tc?
29	805	1.0	2813	"	"	MgO,MnO,SiO_2,H_2O	Opx+Q
35	800	1.0	5355	"	"	MgO,MnO,SiO_2,H_2O	Opx+Q
36	656	1.0	7907	"	"	Opx+Q,H_2O	Opx+Q
33	813	1.0	1156	"	0.428	MgO,MnO,SiO_2,H_2O	Cpx,Qtz
34	816	1.0	1988	"	"	"	Cpx+Qtz
40	808	1.0	2065	"	0.500	MgO,MnO,SiO_2,H_2O	Cpx
32	815	1.0	1156	"	0.571	MgO,MnO,SiO_2,H_2O	Cpx,Pxm,Qtz
38	860	1.0	1508	"	"	"	Cpx,Pxm,Qtz
39	860	1.0	1508	"	0.714	MgO,MnO,SiO_2,H_2O	Pxm
41	800	1.0	3526	"	"	"	
49	795	2.0	1413	"	1.000	MgO,SiO_2,$MnCl_2$	Rhod
67	645	2.0	130	"	"	MnO,SiO_2,H_2O	Pxm
130	463	2.0	1901	NNO,OH(X,G,COH)	"	Pxm	Pxm,Carb,Qtz
Hy-4	800	2.0	72	IW,OH(X,OH)	1.000	MnO,SiO_2,H_2O	Pxm
Hy-5	770	2.0	142	Pt capsule	"	"	Pxm
Hy-9	700	2.0	189	Pt "	"	"	Pxm
Hy-18	714	2.0	168	Pt capsule	"	"	Pxm
Hy-19	712	2.0	92	"	"	"	Pxm
Hy-32	685	2.0	142	Au capsule	"	"	Pxm
Hy-40	327	2.0	1100	MnO,Mn_3O_4,OH(X,OH)	"	Pxm,H_2O	Pxm
Hy-59	656	1.0	1186	G,CH_4(X,OH)	"	MnO,SiO_2,H_2O	Pxm
Hy-69	814	1.0	792	Au capsule	"	"	Rhod
Hy-71	350	2.0	2543	"	"	Pxm,H_2O	Pxm
Hy-73	399	2.0	2543	"	"	"	Pxm
Hy-75	452	2.0	2543	"	"	MnO,SiO_2,H_2O	Pxm

synthesized in two runs at about 800°C; in one of these runs, large rhodonite crystals (1–3 mm) crystallized in a flux of $MnCl_2$. The effect of Mg-bearing component on the pyroxmangite-rhodonite transition was not explored. At lower temperature and/or higher water pressures, manganese-poor compositions contained amphibole. With increasing temperature this amphibole decomposed to orthopyroxene + quartz (runs #18, #22, and #24 in Table 1). Amphibole grew from the higher temperature assemblage in run #31.

X-ray patterns of the products of high temperature runs having bulk Mn/(Mn + Mg) equal to 0.000, 0.143, 0.286, 0.427, 0.500, 0.714, and 1.000 could each be indexed on the basis of a single metasilicate structure type (accompanied by quartz for the amphibole bulk compositions). Only the bulk composition $X = 0.571$ resulted in an X-ray pattern that was obviously a mixture of two metasilicates, kanoite and pyroxmangite. Unit cell dimensions for metasilicate phases in selected runs are given in Table 2. The orthopyroxene cells have very small standard errors and the kanoite cell parameters are precise. The pyroxenoid cell parameters are less precise. Most troubling is the fact that small systematic changes in the positions of reflections result in a relatively large change in the large c di-

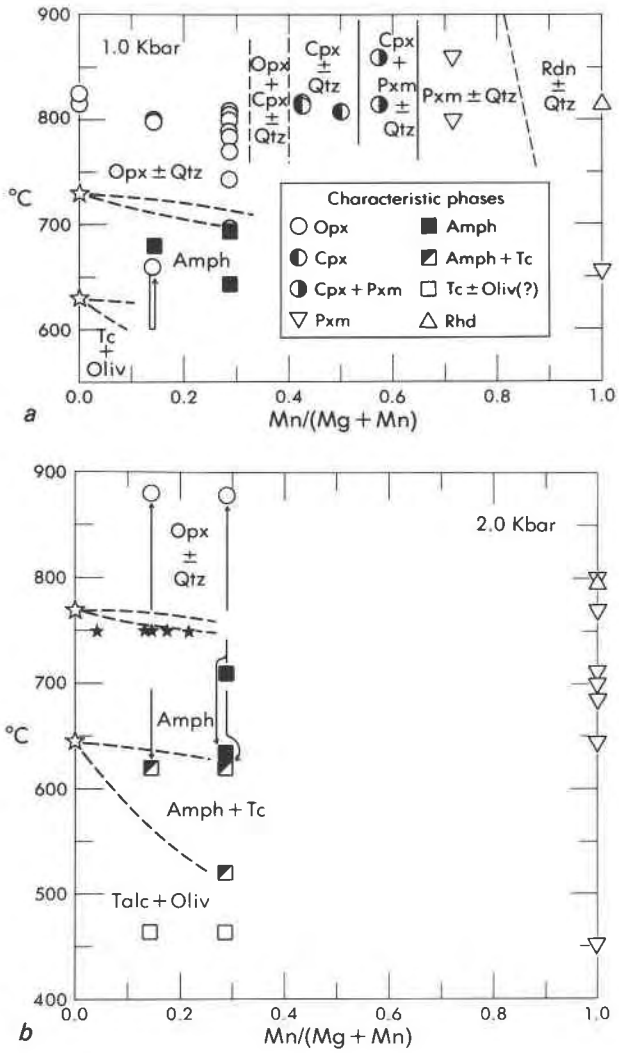

Fig. 1. Characteristic phases grown at various temperatures and at 1.0 and 2.0 kbar water pressure. Abbreviations are: Opx (orthopyroxene), Cpx (the clinopyroxene, kanoite), Rhd (rhodonite), Pxm (pyroxmangite), Amph (amphibole, most likely clinoamphibole), Tc (talc), and Qtz (quartz). The dashed lines suggest how the phase equilibrium boundaries might look, had these boundaries been determined by reversed experiments. The open stars are the positions of univariant reactions determined by Hemley et al. (1977) and the closed stars represent conditions at which Maresch and Czank (1983) synthesized orthoamphibole. In Figure 1b, the arrows indicate the thermal history and the symbol is at the last temperature, before quenching.

mension of the refined unit cell. Part of the problem undoubtedly is due to the small number of single peaks, the low values of l in the indices (hkl) of the reflections used in the refinement, and the possibility that some reflections, which were thought to be uniquely indexed, are actually composite reflections.

Substitution of the Mn component increases the orthopyroxene unit cell size in a regular manner (Fig. 2). The kanoite cell dimensions change only slightly with composition, increasing in size as Mn substitutes for Mg (Table 2). Addition of Mg-component causes the pyroxmangite reflections to shift markedly towards smaller 2θ values. By extrapolating the relationship between composition and the position of major reflections, it is possible to estimate the compositions of the kanoite and pyroxmangite which coexist in the two-phase region at 840°C: X = 0.55 and 0.64 for kanoite and pyroxmangite, respectively (Fig. 3). We will see below that the results of microprobe analysis confirm the X-ray determination of composition for pyroxmangite, but not the coexisting kanoite.

Mixes of amphibole bulk composition run at less than 700°C yielded amphibole, sometimes accompanied by talc and/or olivine. The proportion of talc was greatest in the lowest temperature runs and the runs of shortest duration. X-ray patterns of the amphibole could not be identified with certainty because few reflections were present in the patterns and because the patterns of cummingtonite and anthophyllite (Cameron, 1975, p. 379) are similar. These patterns were best indexed by comparison with the pattern for manganoan cummingtonite (Klein, 1964). The optical extinction angle for this amphibole is between 5 and 15°, supporting its identification as a clinoamphibole. The reflection at 4.7 Å, noted by Maresch and Czank (1983, p. 746), is present in several runs.

Under the microprobe beam, the fluorescence of the metasilicate run products competes in intensity with that of benitoite. Enstatite fluoresces a bright cobalt-blue; perhaps the activator is a trace of cobalt that diffused from the walls of the stellite pressure-vessel (a cobalt alloy), through the wall of the gold capsule, and into the charge during long runs. The manganese-bearing orthopyroxene and kanoite fluoresce a very bright red color. The fluorescence of pyroxmangite is an orange-red color that is not as bright as that of the pyroxenes. The rhodonite, grown in $MnCl_2$ flux, fluoresces brilliant red, similar in behavior to the manganiferous pyroxenes. No phosphorescence was noted.

Microprobe analysis of the orthopyroxene confirms that most products have a bulk composition that, within the limits of analytical error (1% of the Mn/(Mn + Mg)), is homogeneous and equal to the intended composition of the starting mixes (Fig. 4). However, analysis of run #39, with composition Mn/(Mn + Mg) = 0.714 and whose X-ray powder diffraction pattern consists only of sharp reflections of magnesian pyroxmangite, yielded a cluster of points at 0.715, additional points within the region inferred from the X-ray diffraction results to be that of pyroxmangite (0.63 to 0.69), and two points at 0.42 (magnesian kanoite). Analysis of run #32, with composition Mn/(Mn + Mg) = 0.571, shows clusters of points at 0.62–0.69 (confirming the composition of 0.64 determined by the X-ray diffraction method), 0.42–0.52, and 0.27–0.34. These composition ranges are similar to those previously inferred for magnesian-pyroxmangite, kanoite, and orthopyroxene. Likewise, run #34 with an intended bulk composition of 0.43 has analytical points ranging from 0.17 to 0.44. The analytical uncertainty associated

Table 2. Unit cell dimensions of (Mn,Mg)SiO_3 phases

Run#	Phase	$\frac{Mn}{(Mn+Mg)}$	σ x100	a,Å	b,Å	c,Å	α,°	β,°	γ,°	R*
43	Opx	0.0	1.5	18.225(2)	8.818(1)	5.178(1)				37
45	Opx	0.0	1.7	18.223(2)	8.818(1)	5.179(1)				37
				18.227(2)	8.818(1)	5.180(1)				39
10	Opx	0.143	1.8	18.290(3)	8.849(1)	5.206(1)				28
12	Opx	0.143	1.3	18.292(2)	8.848(1)	5.203(1)				29
30	Opx	0.143	2.0	18.291(3)	8.850(1)	5.201(1)				31
37	Opx	0.143	1.2	18.289(2)	8.846(1)	5.202(1)				29
11	Opx	0.286	1.7	18.350(2)	8.879(1)	5.221(1)				26
29	Opx	0.286	1.8	18.352(3)	8.876(2)	5.223(2)				24
35	Opx	0.286	1.7	18.352(2)	8.878(1)	5.225(1)				25
36	Opx	0.286	1.2	18.352(2)	8.875(1)	5.227(1)				20
34	Kan	0.428	2.2	9.724(3)	8.911(2)	5.247(2)		108.60(3)		17
40	Kan	0.500	1.8	9.732(2)	8.934(1)	5.245(2)		108.52(2)		21
39	Pxm	0.714	1.4	6.672(2)	7.528(2)	17.350(3)	113.77(2)	81.96(2)	94.63(2)	19
			1.0	6.661(1)	7.522(1)	17.326(5)	113.78(2)	82.10(2)	94.62(2)	20
41	Pxm	0.714	1.8	6.664(2)	7.524(2)	17.346(4)	113.77(2)	81.95(3)	94.66(2)	24
			1.8	6.673(1)	7.528(2)	17.351(4)	113.73(2)	82.01(2)	94.56(2)	29
67	Pxm	1.000	1.7	6.717(2)	7.601(2)	17.429(11)	113.79(3)	82.35(5)	94.73(3)	15
130	Pxm	1.000	3.0	6.712(4)	7.603(3)	17.443(19)	113.73(5)	82.40(9)	94.68(5)	17
		1.000	1.6	6.718(1)	7.598(1)	17.469(7)	113.80(2)	82.28(3)	94.68(2)	27
49	Rhd	1.000	3.0	7.614(3)	11.856(6)	6.703(2)	92.40(4)	94.25(4)	105.73(4)	24
69	Rhd	1.000	1.7	7.620(1)	11.852(2)	6.704(1)	92.48(2)	94.38(1)	105.65(1)	33

*R is the number of reflections accepted during the refinement.

with the scattered points in runs #34 to #32 is difficult to assess because the run products are intergrowths of small subhedral grains, but this compositional dispersion is believed to be real for two reasons. (1) The analytical sums and values for silicon were not dependent on the Mn/Mg ratio, which would be the case if the X-ray activation volume were to include part of the epoxy mounting medium. (2) The scattered points do not cluster symmetrically about a mean value. These results suggest that even in long runs, compositional homogeneity is not achieved. The fact that analyses of a single run cluster about two or three mean compositions (Fig. 4) suggests that several distinct compositions or phases are being analyzed. It is possible that the first assemblage to crystallize is not the stable assemblage, but that these first-formed phases are remarkably persistent, even in a hydrothermal environment.

Discussion of results

Unit cell dimensions of metasilicates obtained in this study agree reasonably well with those for synthetic enstatite (Turnock et al., 1973), pyroxmangite (Maresch and Mottana, 1976; Ito, 1972), rhodonite (Ito, 1972), natural kanoite (Kobayashi, 1977) and donpeacorite (Petersen et al., 1984), but there are some subtle differences that merit discussion. The cell dimensions of the new orthopyroxene, donpeacorite, can be plotted on diagrams of composition versus cell edge of Mn-Mg orthopyroxene measured in this study (Fig. 2). The b and c cell edges of natural donpeacorite suggest that its composition is $X = 0.29$, in good agreement with the microprobe analysis of Petersen et al. (1984). However, their a cell dimension of the natural pyroxene is too large to be consistent with the other dimensions. Natural donpeacorite is very pure; the minor amount of CaO in the analysis cannot be expected to expand the a dimension from 18.351 Å in synthetic donpeacorite of composition $X = 0.29$ to the value of 18.384 Å observed for the natural sample. This change is equivalent to 3 times the uncertainty ($\sigma = 0.011$ Å) reported by Petersen et al. (1984). There remain two possible causes for the apparent discrepancy in the value of the a cell edge: systematic error in a alone, or changes in a brought about by a difference in structural state. The close agreement between the observations of the b and c dimensions of the natural and synthetic samples would suggest that the difference in a is not due to systematic error that similarly effects all three lattice constants. On the other hand, the structure refinement of the natural donpeacorite

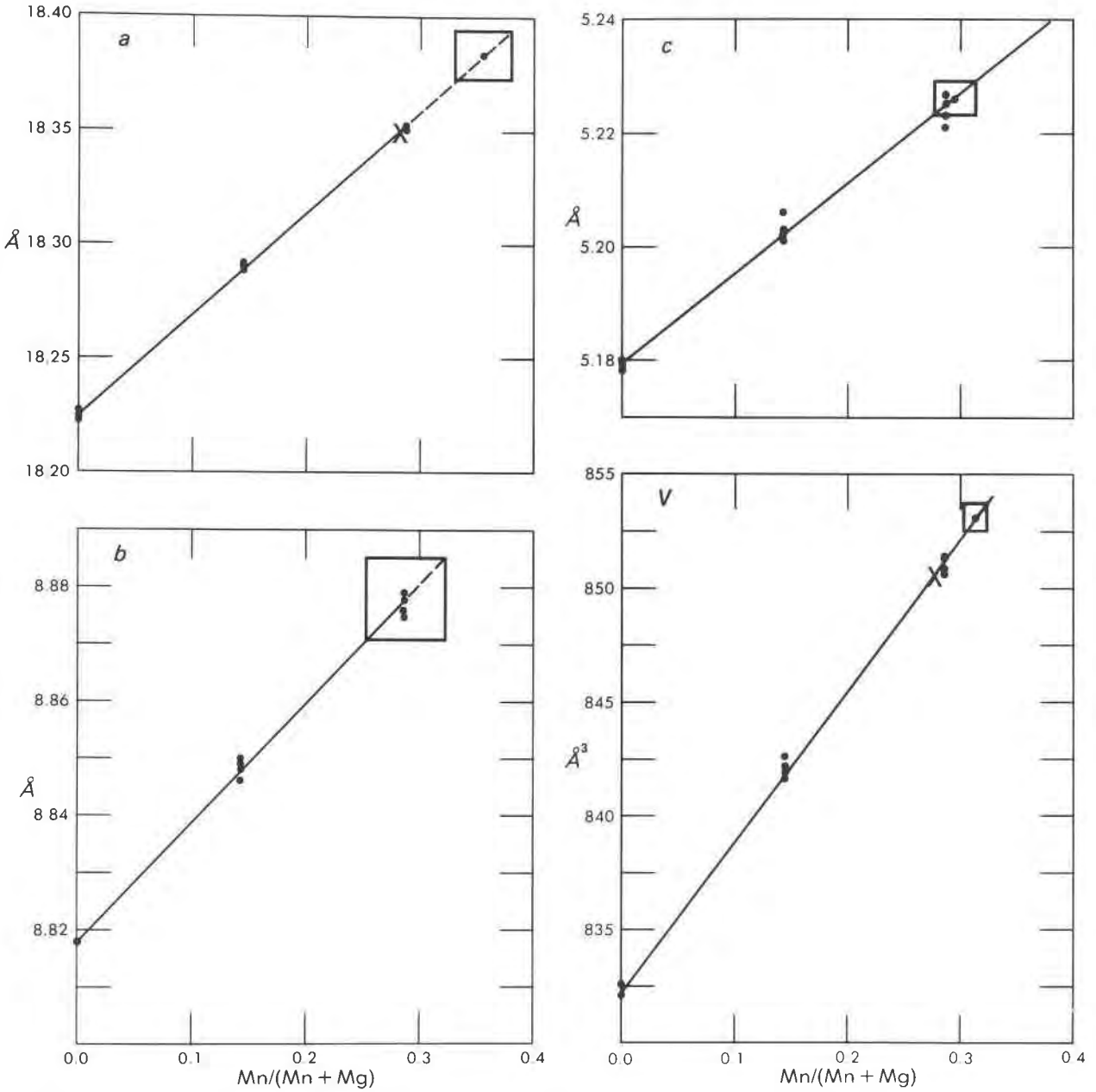

Fig. 2. Unit cell dimensions of synthetic orthopyroxenes in the system $MgSiO_3$-$MnSiO_3$ plotted against composition. The dimensions of natural donpeacorite (Petersen et al., 1984) are plotted as rectangles on the straight-line relationship derived from the synthetic orthopyroxenes. The height of the rectangle is the uncertainty in a cell dimension quoted by Petersen et al. (1984); the width is the corresponding uncertainty in composition. Compositions determined from the *b* and *c* dimensions reported by Petersen et al. (1984), but not their values for the *a* dimension or *V*, are in good agreement with the reported composition of Mn/(Mn + Mg) = 0.29 determined by electron microprobe analysis. The revised values of *a* and *V* (Table 3), shown as crosses (X), bring about excellent agreement between all cell dimensions of the natural material and its reported composition.

indicates that all of the Mn is situated in the M(1) site (Petersen et al., 1984), an observation that is consistent with the ordering of cations during slow cooling of a metamorphic terrane. In contrast, the Mg-Mn orthopyroxenes synthesized at high temperatures were quenched rapidly in the laboratory, a procedure that could produce a disordered orthopyroxene. The ordering process is one that moves the larger Mn cations (effective ionic radius 0.83 Å; Shannon, 1976) from the larger 8-fold M(2) site to the octahedral M(1) site, and moves an identical number of

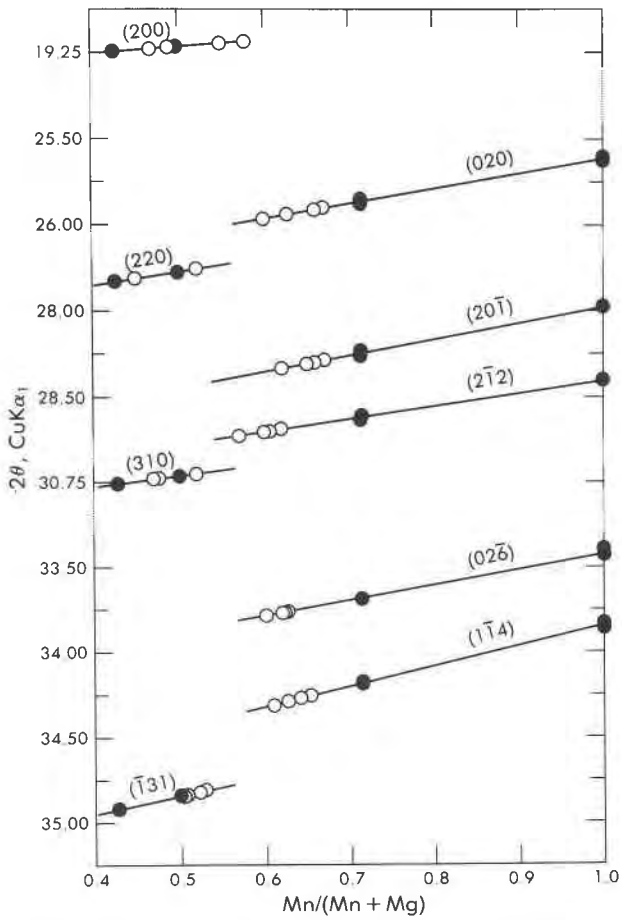

Fig. 3. Composition versus 2θ for various X-ray diffraction reflections calculated (filled circles) from refined unit cell dimensions of kanoite (left) and pyroxmangite (right). Measured 2θ values (open circles) are for kanoite and pyroxmangite reflections observed in runs #32 and #39, each with a bulk composition of Mn/(Mn + Mg) = 0.571. The compositions of coexisting kanoite and pyroxmangite appear to be close to 0.50 and 0.64.

smaller Mg cations (radius 0.72 Å) in the opposite direction. Hawthorne and Ito (1977, their Fig. 6) have determined the mean ⟨M-O⟩ bond length for the M(1) and M(2) sites as a function of the mean radius of the constituent cations. On going from a completely disordered to a completely ordered state of donpeacorite, the mean ⟨M2-O⟩ distance increases 0.04 Å, from 2.19 to 2.23 Å, while the ⟨M1-O⟩ decreases from 2.105 to 2.075 Å. Ad-

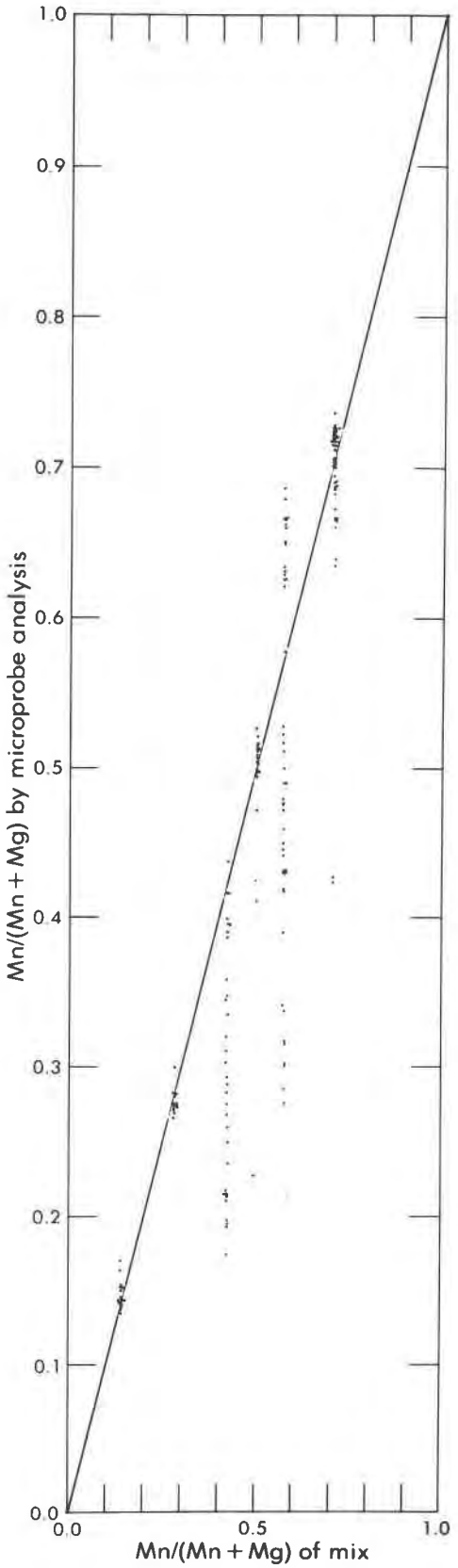

Fig. 4. Weighed compositions of mixes plotted against the atomic ratio Mn/(Mg + Mn) for individual microprobe analyses of grains in the run products. The bulk composition of single phase (by X-ray powder diffraction methods) run products reflects that of the mix. Runs which showed two distinct phases in the X-ray patterns were found to be heterogeneous by microprobe analysis.

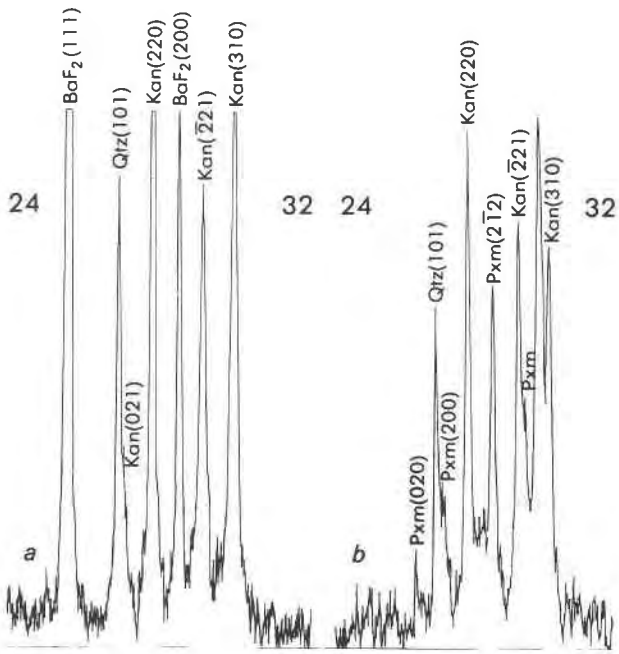

Fig. 5. Routine X-ray powder diffraction patterns of (a) run #34 (kanoite + quartz, amphibole bulk composition with Mn/(Mg + Mn) = 0.43) and (b) #32 (kanoite + pyroxmangite + quartz, amphibole bulk composition with Mn/(Mg + Mn) = 0.57). Both patterns were made using Cu$K\alpha$ radiation over the 2θ range 24 to 32°. Although the metasilicate reflections appear as sharp as those of quartz and the BaF_2 internal standard, microprobe analyses (Fig. 4) indicate that these metasilicates are not compositionally homogeneous.

jacent M1 and M2 sites lie in a plane perpendicular to **a**, separating the tetrahedral chains (see Fig. 12 of Cameron and Papike, 1980). If the larger or M2 site determines the spacing between the chains, the ordering process would expand the a dimension. The ordering hypothesis could be proved or disproved by comparing the cell dimensions of annealed, rapidly quenched donpeacorite with the cell dimension of material that had not been annealed.

To determine the cause of the discrepancy in the a cell dimension (systematic error in the measurement of a or difference in thermal history), the unit cell dimensions of the natural donpeacorite were redetermined. Small fragments of resinous brown pyroxene were handpicked to separate them from most of the associated amphibole. These fragments were crushed to pass a 250 μm screen; most of the remaining amphibole passed through a 149 μm screen, leaving behind a fraction (150–250 μm) concentrated in pyroxene. This pyroxene-rich fraction was ground, then mixed with about 5 volume-percent BaF_2 internal standard, and peak positions were measured as described by Huebner and Papike (1970). Thirty-eight reflections (Table 3) were indexed by comparison with the hypersthene pattern calculated by Borg and Smith (1969, p. 275) and with a donpeacorite pattern calculated by Howard T. Evans, Jr., using the structural parameters of Petersen et al. (1984). Thirty-four unambiguously indexed reflections were used to obtain the cell dimensions a = 18.350(2) Å, b = 8.867(1) Å, and c = 5.227(1) Å, in good agreement with the four values for synthetic orthopyroxene of similar composition (Table 2). Evidently there is a systematic error in the original determination of a by Petersen et al. (1984), perhaps due to their use of only 9 reflections in their refinement. Furthermore, we can conclude that the disparate thermal histories of the synthetic and natural donpeacorite do not bring about a significant difference in the lattice constants of this phase.

The existence of pyroxenoids with a repeat distance greater than 7 tetrahedra along the tetrahedral chains was not demonstrated, but such negative evidence does not preclude their existence. If actually present, such phases might help explain the large range of compositions found in certain runs, particularly runs #32 and #34. Compositions in the range 0.40 to 0.70 should be reinvestigated by the techniques of transmission electron microscopy to verify that the grains are solely kanoite and pyroxmangite and, if not, to reveal all of the structures that are present.

The spread of microprobe analyses for compositions

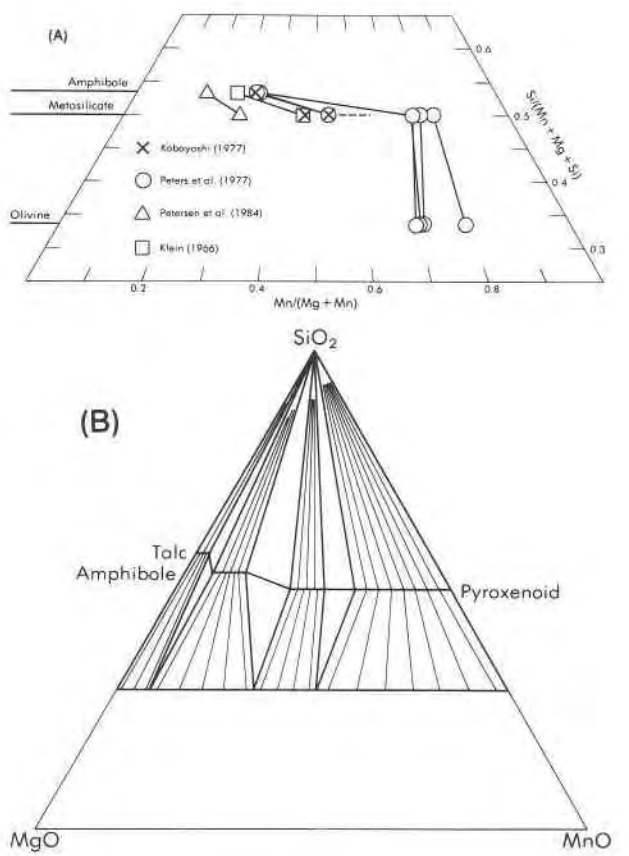

Fig. 6. Quaternary phase compatibility diagrams, projected from H_2O vapor onto the plane MnO-MgO-SiO_2. Figure 6a shows the relevant natural assemblages described by Klein (1966), Peters et al. (1977), Kobayashi (1977), and Petersen et al. (1984). Each occurrence is discussed in the text. Figure 6b shows the proposed phase assemblages at 600°C and 4.5 kbar pressure for compositions more siliceous than olivine.

Table 3. X-ray powder diffraction data for donpeacorite

hkl	d(obs.)	d(calc.)	I(obs.)
*	4.504		2
	4.172		1
211	4.039		3
121	3.322	3.324	8
*	3.256		9
*	3.248		9
420	3.1888	3.1883	100
*	3.0710		12
321	2.9594	2.9587	24
610	2.8916	2.8916	69
511	2.8448	2.8446	17
*	2.7946		1
*	2.7840		2
*	2.7697		2
421	2.7205	2.7215	21
	2.5938		2
131	2.5477	2.5476	21
611	2.5303	2.5299	10
202	2.5131	2.5122	13
521	2.4858	2.4865	15
231	2.4795	2.4770	13
302	2.4005		2
711	2.2646	2.2655	5
431	2.2425	2.2441	1
	2.1667		3
	2.1644		3
502	2.1277	2.1282	10
531	2.1065	2.1068	14
721	2.0718	2.0717	4
820	2.0384		4
	2.0319		4
141	2.0285	2.0284	6
440	1.9961	1.9960	10
241	1.9922	1.9920	10
631	1.9697	1.9688	14
821	1.8991	1.8982	3
702	1.8509	1.8504	3
10.10	1.7964	1.7972	7
250	1.7408	1.7412	7
722	1.7079	1.7077	3
812	1.6933		2
*	1.6474		8
023	1.6220	1.6217	2
123	1.6157	1.6154	4
931	1.5979	1.5980	5
650	1.5345	1.5342	4
12.00	1.5296	1.5294	5
133,10.31	1.4946		12
060	1.4775	1.4778	11
352	1.4275	1.4270	5
11.02	1.4060	1.4061	4
11.31	1.3999	1.3998	9

$\underline{a}$ = 18.350(2) Å
$\underline{b}$ = 8.867(1)
$\underline{c}$ = 5.227(1)
$\underline{V}$ = 850.6(2) Å^3

$Mn/(Mn + Mg) = 0.571$ and 0.714 was not expected in such long runs and may not be correctly dismissed as simply reflecting compositions that nucleated early and persisted during the rest of the experiment. It would be informative to repeat these experiments using gel starting materials, such as those used by Maresch and Czank (1983). Gels might provide a greater nucleation density than the oxide mixes, perhaps resulting in a finer grain size and therefore a greater opportunity for compositional equilibrium.

It is noteworthy that, when synthesizing amphiboles, Maresch and Czank (1983) encountered the same difficulties that plagued the early parts of this study. Although they used gels as starting materials, they too found that in most cases talc, pyroxene, and other phases coexisted with amphibole. The use of gels might also explain the formation of the predominantly orthorhombic amphibole run product observed by Maresch and Czank (1983), as

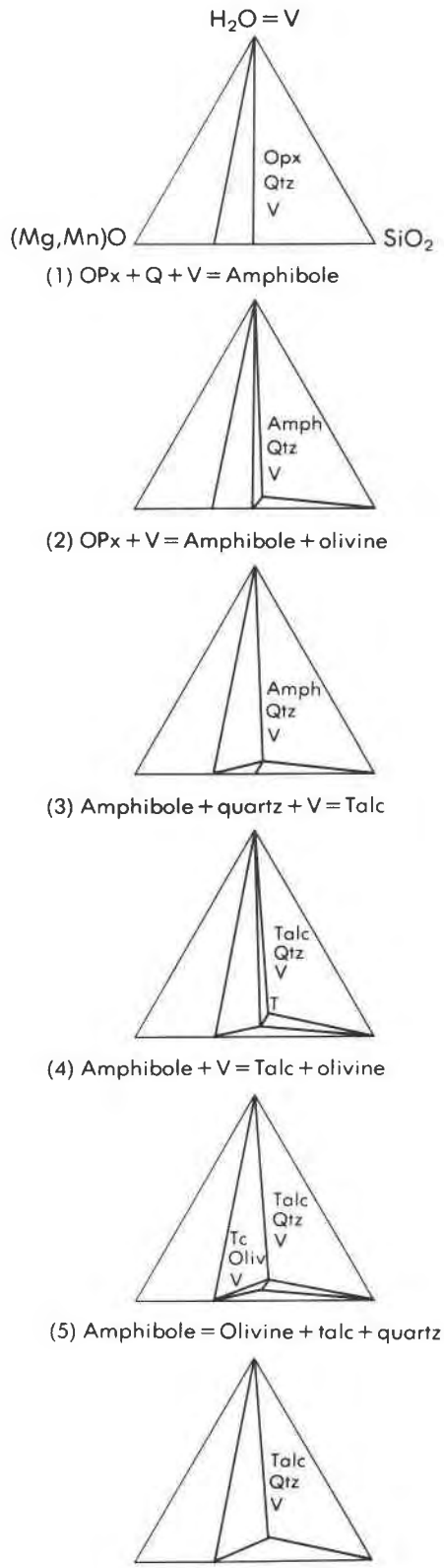

Fig. 7. Phase compatibility fields for the pseudo-ternary system (Mn,Mg)O-SiO_2-H_2O. Abbreviations are Q or Qtz for quartz, Oliv for olivine, OPx for orthopyroxene, Amph for amphibole, and T or Tc for talc, and V for vapor. Reactions (1) and (4) bound the amphibole field shown in Figure 1.

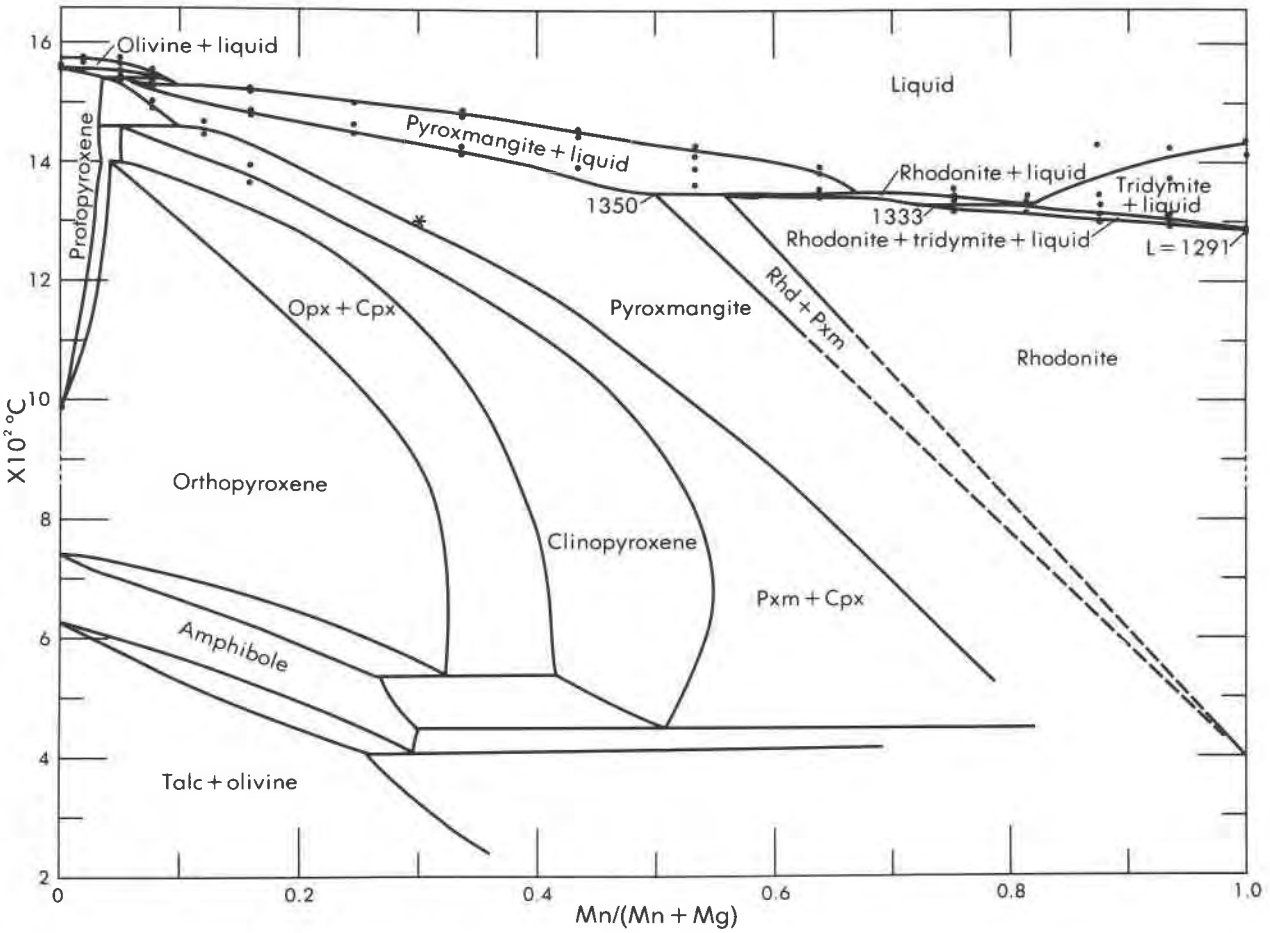

Fig. 8. One set of possible phase relations for the system $MgSiO_3$-$MnSiO_3 \pm (SiO_2, H_2O)$. An isobaric section for metasilicate bulk composition at temperatures above the amphibole stability range has been drawn using data from Glasser and Osborn (1960), Ito (1972) and Figure 1 of the present study. The runs of Glasser and Osborn (small, solid circles) are consistent with the phase boundaries in this figure if their clinopyroxene was either stable or formed from protoenstatite on quenching, and if their magnesian rhodonite was in reality the magnesian pyroxmangite reported by Ito (1972). For the temperature range at and below which amphibole is stable, the bulk composition is amphibole and the fields are based on the natural assemblages discussed in the text, the work of Hemley et al. (1977), and Figure 1. The asterisk (*) indicates a single run in which kanoite reacted totally to pyroxmangite, indicating that pyroxmangite is stable relative to the clinopyroxene at this composition and 1300°C.

opposed to the monoclinic amphibole identified in the present study.

Petrologic inferences

Although phase compatibility relations for manganiferous metasilicates at intermediate to high grade metamorphic conditions have been proposed by Brown et al. (1980) and Petersen et al. (1984) using the compositions of coexisting natural minerals, the relationship between these phases and amphibole is not well known. In Figure 6, I attempt to portray the tie-line orientations between amphibole, metasilicate, and olivine for minerals that have compositions rich in MgO and MnO, yet poor in FeO, CaO, Na_2O, and Al_2O_3. There are few reports of analyzed assemblages with such bulk compositions, but four occurrences proved informative (Fig. 6a). First, Petersen et al. (1984) give the analysis of "tirodite" amphibole with 4.8% CaO that coexists with the donpeacorite previously discussed, in upper amphibolite facies siliceous marbles metamorphosed at 650±50°C and 6.5±1.0 kbar. Second, Kobayashi (1977) gives analyses of coexisting cummingtonite and kanoite. He states that pyroxmangite is also present and that the metamorphic grade is that of the hornblende hornfels facies. Third, Klein (1966, his assemblage 5) reports analyses of Mn-cummingtonite, magnesioriebeckite, and Ca-poor rhodonite that coexist with hematite and talc in an unusual kyanite zone rock. The rhodonite is extraordinarily magnesian, more so than any pyroxenoid plotted by Brown et al. (1980). Klein's "rhodonite" might actually be the clinopyroxene kanoite, which has a similar composition and was not described until 11 years later (Kobayashi, 1977). Finally, Peters et al. (1977) report analyses of coexisting Mn-cummingtonite, pyroxenoid, and tephroite that were metamorphosed at

550±50°C and 3 kbar. As in the previous case, one "pyroxmangite" (B-5-22 - 64.6 IV) has the composition of kanoite and might be the clinopyroxene, rather than pyroxenoid. In Figure 6b I have combined all relevant information to show the composition fields as they might exist at 600°C and 4.5 kbar.

The two reactions that bound the amphibole field as suggested in Figure 1 can best be understood in terms of the pseudoternary system (Mn,Mg)O-SiO_2-H_2O. With decreasing temperature, orthopyroxene, quartz, and vapor of amphibole *Bulk* composition react to form cummingtonite or anthophyllite:

$$7(Mn,Mg)_2Si_2O_6 + 2SiO_2 + 2H_2O = 2(Mn,Mg)_7Si_8O_{22}(OH)_2$$

At lower temperature, amphibole breaks down to form talc and olivine:

$$10(Mn,Mg)_7Si_8O_{22}(OH)_2 + 8H_2O = 8(Mn,Mg)_2SiO_4 + 9(Mn,Mg)_6Si_8O_{20}(OH)_4$$

However for compositions that depart from amphibole *Bulk* composition, 5 reactions (Fig. 7) are necessary.

Possible phase relations of some (Mn,Mg)-silicates are shown in Figure 8, which incorporates the liquidus phase relations at one bar (Glasser and Osborn, 1960), the results of Ito (1972) at 1300°C, the findings of the current study at 500–850°C and 1 kbar, and the compositions of Mn-Mg minerals which coexist in nature at higher pressures. The water fugacity is assumed to be sufficiently great for the formation of amphibole and talc, but the phase boundaries are assumed to be independent of pressure. The most striking feature of the diagram is the presence, at high temperature, of pyroxmangite at compositions normally associated with orthopyroxene. The termination of kanoite near the solidus is uncertain because this phase was not known to exist when the earlier studies were made. One new datum is the reaction of kanoite to form pyroxmangite at 1300°C (Fig. 8); at this composition and temperature, at least, the pyroxenoid is more stable than clinopyroxene. The reaction is too sluggish at 1200 to 1250°C to be easily reversed.

No effort was made in this study to synthesize amphiboles with greater than 2 Mn cations per formula unit because, at the time of the experiments, it was thought that Mn could occupy only the two M(4) sites (which are filled by calcium ions in the tremolite-actinolite amphiboles). However, the two cummingtonites analysed by Peters et al. (1977) each contain 2.3 Mn cations and 0.1 calcium cations per formula unit based on 15 cations; evidently manganese can also occupy other sites (M(1)–M(3)) in amphibole.

Acknowledgments

As a result of reviewing a manuscript version of this paper for the journal, Donald R. Peacor (University of Michigan) provided chips from the original donpeacorite specimen so that the ordering hypothesis could be tested. Howard T. Evans, Jr., kindly confirmed the surprising result of the redetermination of the donpeacorite cell dimensions and provided a calculated powder pattern. The manuscript also benefitted from reviews by Julian J. Hemley and Richard A. Robie (U.S. Geological Survey) and Cornelis Klein (University of New Mexico).

References

Albee, A. L. and Ray, Lily (1970) Correction factors for electron probe microanalysis of silicates, oxides, carbonates, phosphates, and sulfates. Analytical Chemistry, 42, 1408–1414.

Akimoto, Syun-iti and Syono, Yasuhiko (1972) High pressure transformations in $MnSiO_3$. American Mineralogist, 57, 76–84.

Bence, A. E. and Albee, A. L. (1968) Empirical correction factors for the electron microanalysis of silicates and oxides. Journal of Geology, 76, 382–403.

Borg, I. Y. and Smith, D. K. (1969) Calculated X-ray powder patterns for silicate minerals. Geological Society of America Memoir 122.

Brown, P. E., Essene, E. J., and Peacor, D. R. (1980) Phase relations inferred from field data for Mn pyroxenes and pyroxenoids. Contributions to Mineralogy and Petrology, 74, 417–425.

Cameron, K. L. (1975) An experimental study of actinolite-cummingtonite phase relations with notes on the synthesis of Fe-rich anthophyllite. American Mineralogist, 60, 375–390.

Cameron, Maryellen and Papike, J. J. (1980) Crystal chemistry of silicate pyroxenes. In C. T. Prewitt, Ed., Reviews in Mineralogy, Vol. 7: Pyroxenes, p. 5–92. Mineralogical Society of America, Washington, D.C.

Evans, H. T., Jr., Appleman, D. E., and Handwerker, D. S. (1963) The least squares refinement of crystal unit cells with powder diffraction data by an automatic computer indexing method. American Crystallographic Association Annual Meeting Program, 42–43.

Finger, L. W. and Hadidiacos, C. G. (1972) Electron microprobe automation. Carnegie Institution of Washington Yearbook, 71, 598–600.

Glasser, F. P. and Osborn, E. F. (1960) The ternary system MgO–MnO–SiO_2. Journal of the American Ceramic Society, 43, 132–140.

Gordon, W. A., Peacor, D. R., Brown, P. E., and Essene, E. J. (1981) Exsolution relationships in a clinopyroxene of average composition $Ca_{0.43}Mn_{0.69}Mg_{0.82}Si_2O_6$: X-ray diffraction and analytical electron microscopy. American Mineralogist, 66, 127–141.

Hawthorne, F. C. and Ito, Jun (1977) Synthesis and crystal-structure refinement of transition-metal orthopyroxenes. 1: Orthoenstatite and (Mg, Mn, Co) orthopyroxene. Canadian Mineralogist, 15, 321–338.

Hemley, J. J., Montoya, J. W., Shaw, D. R., and Luce, R. W. (1977) Mineral equilibria in the MgO-SiO_2-H_2O system: II Talc-antigorite-forsterite-anthophyllite-enstatite stability relations and some geologic implications in the system. American Journal of Science, 277, 353–383.

Huebner, J. S. (1967) Stability Relations of Minerals in the System Mn-Si-C-O. Ph.D. Thesis, The Johns Hopkins University, Baltimore.

Huebner, J. S. (1969) Stability relations of rhodochrosite in the system manganese-carbon-oxygen. American Mineralogist, 54, 457–481.

Huebner, J. S. (1971) Buffering techniques for hydrostatic systems at elevated pressures. In G. C. Ulmer, Ed., Research Techniques for High Pressure and Temperature, p. 123–177. Springer Verlag, New York.

Huebner, J. S. and Papike, J. J. (1970) Synthesis and crystal chemistry of sodium-potassium richterite, $(Na,K)NaCaMg_5Si_8O_{22}(OH,F)_2$: a model for amphiboles. American Mineralogist, 55, 1973–1992.

Ito, Jun (1972) Rhodonite-pyroxmangite peritectic along the join $MnSiO_3$-$MgSiO_3$ in air. American Mineralogist, 57, 865–876.

Klein, Cornelis, Jr. (1964) Cummingtonite-grunerite series: a chemical, optical and X-ray study. American Mineralogist, 49, 963–982.

Klein, Cornelis, Jr. (1966) Mineralogy and petrology of the metamorphosed Wabush Iron Formation, southwestern Labrador. Journal of Petrology, 7, 246–305.

Kobayashi, Hideo (1977) Kanoite, $(Mn^{2+},Mg)_2[Si_2O_6]$, a new clinopyroxene in the metamorphic rock from Tatehira, Oshima Peninsula, Hokkaido, Japan. Journal of the Geological Society of Japan, 83, 537–542.

Maresch, W. V. and Czank, Michael (1983) Phase characterization of synthetic amphiboles on the join Mn_x^{2+} Mg_{7-x} $[Si_8O_{22}]$ $(OH)_2$. American Mineralogist, 68, 744–753.

Maresch, W. V. and Mottana, A. (1976) The pyroxmangite-rhodonite transformation for the $MnSiO_3$ composition. Contributions to Mineralogy and Petrology, 55, 69–79.

Peters, Tj., Valarelli, J. V., Coutinho, J. M. V., Sommerauer, J., and von Raumer, J. (1977) The manganese deposits of Buritirama (Pará, Brazil). Schweizerische Mineralogische und Petrographische Mitteilungen, 57, 313–327.

Petersen, E. U., Anovitz, L. M., and Essene, E. J. (1984) Donpeacorite, $(Mn,Mg)MgSi_2O_6$, a new orthopyroxene and its proposed phase relations in the system $MnSiO_3$-$MgSiO_3$-$FeSiO_3$. American Mineralogist, 69, 472–480.

Robinson, Peter (1980) The composition space of terrestrial pyroxenes—internal and external limits. In C. T. Prewitt, Ed., Reviews in Mineralogy, Vol. 7: Pyroxenes, p. 419–494. Mineralogical Society of America, Washington, D.C.

Shannon, R. D. (1976) Revised effective ionic radii and systematic studies of interatomic distances in halides and chalcogenides. Acta Crystallographica, A32, 751–767.

Turnock, A. C., Lindsley, D. H., and Grover, J. E. (1973) Synthesis and unit cell parameters of Ca-Mg-Fe pyroxenes. American Mineralogist, 58, 50–59.

Manuscript received, March 21, 1985;
accepted for publication, September 22, 1985.